Ab-initio calculations of structural, phonon and thermal properties of $Al_xGa_{1-x}As$ alloy

A FAZELI KISOMI[1] [ORCID],* and S J MOUSAVI[2]

[1]Departemant of Physics, Ardabil Branch, Islamic Azad University, Ardabil, Iran
[2]Department of Physics, Rasht Branch, Islamic Azad University, Rasht, Iran
*Corresponding author. E-mail: alif1364@yahoo.com

Abstract. Structural, phonon and thermal properties of $Al_xGa_{1-x}As$ alloy for different values of x ($x = 0.0$, 0.25, 0.5, 0.75 and 1.0) have been investigated by quasiharmonic Debye–Einstein model and Quantum Espresso package. The correction of Vegard's law for lattice constant has been examined and has a good agreement with other experimental and theoretical works. TO–LO splitting at gamma point, which is related to breaking of cubic symmetry, has been calculated by optical phonon mode calculation. It is found that by increasing the amount of Al in $Al_xGa_{1-x}As$ alloy, specific heat at constant pressure and Debye temperature will be increased.

Keywords. *Ab-initio* calculations; $Al_xGa_{1-x}As$; thermal properties and quasiharmonic Debye–Einstein model.

PACS Nos 65.40.−b; 63.20.dk

1. Introduction

Group III–V compounds are one of the most important semiconductor materials because of their applications in electronic and optoelectronic devices [1]. $Al_xGa_{1-x}As$ is the most important and the most studied III–V semiconductor alloy [2]. Structural and electronic properties of $Al_xGa_{1-x}As$ for different values of x have been theoretically investigated by Mao *et al* [1]. The energy levels and the radial probability distributions of an electron with an impurity in a spherical quantum dot which is layered as $GaAs/Al_xGa_{1-x}As/AlAs$ have been calculated by Boz *et al* [3]. Also investigation on structural asymmetry induced size quantised non-monotonous electron mobility in $GaAs/Al_xGa_{1-x}As$ double quantum well structure has been done by Nayak *et al* [4]. $Al_xGa_{1-x}As/GaAs$ heterostructure with abnormally high mobility of charge carriers has been investigated by Seredin *et al* [5].

Investigation of the thermal properties of solids is an old topic which arises in strong connection with the fundamental physical properties of the solids [6]. Investigation on the effect of changing concentration of materials in ternary alloys and effect of that on thermal properties are very popular in computational physics. Investigation on the correction of the Vegard's law [7] in $Al_xGa_{1-x}As$ alloy by quasiharmonic Debye model

by using the computing code GIBBS [8] has been done by El Haj Hassan *et al* [2]. Unfortunately, investigation on the thermal properties of $Al_xGa_{1-x}As$ alloy by Debye–Einstein model was not given much attention. In this paper, we shall try to investigate structural and thermal properties of $Al_xGa_{1-x}As$ for different values of x ($x = 0.0, 0.25, 0.5, 0.75, 1.0$) by quasiharmonic Debye–Einstein model and computing code GIBBS2 [9,10]. Also, phonon properties of optical modes of this alloy will be analysed by density functional perturbation theory (DFPT).

Because of the difficulty of experimental investigation of thermal properties of this alloy and the importance of this alloy, representation of results and comparison of the results with other results will be interesting.

2. Computational details

In this paper, $Al_xGa_{1-x}As$ alloy has been modelled with different values of x ($x = 0.0, 0.25, 0.5, 0.75, 1.0$) in terms of periodically repeated supercells with 8 atoms per unit cell. When $x = 0.25$ and 0.75, we have used eight-atoms simple cubic cell with fewer anions from a regular simple cubic lattice. When $x = 0.5$, a cubic cell containing identical atoms in the same level has been used.

For calculating thermal properties in quasiharmonic Debye–Einstein model, energy–volume data and frequencies of optical modes in equilibrium volume at gamma point are required. Thus, Quantum Espresso package [11] with a cut-off energy of 80 Ryd, uniform k-mesh 7*7*7 and local density approximation (LDA) as an exchange-correlation potential has been used.

For phonon calculations, q-mesh $2 \times 2 \times 2$ has been considered. All the parameters have been optimised.

In quasiharmonic Debye–Einstein model used in the computing code GIBBS2, non-equilibrium functional Gibbs free energy is obtained by

$$G^*(V; P, T) = E(V) + PV + F_{\text{vib}}[\theta_{\text{DE}}(V), T], \quad (1)$$

where $E(V)$ can be obtained by *ab-initio* calculations, p is related to hydrostatic pressure and F_{vib} is the Helmholtz free energy which is obtained by the equation

$$F_{\text{vib}}^* = \int_0^\infty \left[\frac{\omega}{2} + K_B T \ln\left(1 - e^{\omega_i/K_B T}\right) \right] g(\omega) \, d\omega, \quad (2)$$

where $g(\omega)$ is the phonon density of states which is obtained from this relation for Debye–Einstein model:

$$\begin{cases} 9n \dfrac{\omega^2}{\omega_{\text{DE}}^3} & \text{if } \omega < \omega_{\text{DE}} \\ \sum_{j=1}^{3n-3} \delta(\omega - \omega_j) & \text{if } \omega \geq \omega_{\text{DE}} \end{cases} \quad (3)$$

In this relation $\omega_{\text{DE}} = K_B \theta_{\text{DE}}$, where

$$\theta_{\text{DE}} = \frac{\theta_D}{n^{1/3}}. \quad (4)$$

Here n is the number of atoms in the chemical formula and θ_D, the Debye temperature, is obtained by the Slater method

$$\theta_D = \frac{\hbar}{k} [6\pi^2 V^{1/2} N]^{1/3} f(\sigma) \sqrt{\frac{B_s}{M}}. \quad (5)$$

σ is the Poison ratio and the function $f(\sigma)$ is expressed by the following equation. Poison ratio is considered to be about 0.25.

$$f(\sigma)$$
$$= \left\{ 3 \left[2 \left(\frac{2}{3} \frac{1+\sigma}{1-2\sigma} \right)^{3/2} + \left(\frac{1}{3} \frac{1+\sigma}{1-\sigma} \right)^{3/2} \right]^{-1} \right\}^{1/3}. \quad (6)$$

Also, M is the molecular mass of each unit cell and B_s is the adiabatic bulk modulus which determines compressibility of the crystal and is obtained by the equation

$$B_s \cong B_{\text{static}} \left[V \frac{d^2 E}{dV^2} \right]. \quad (7)$$

In relation (3), ω_i is the frequency of optical modes which is obtained by

$$\omega_i(\Gamma) = \omega_i^0(\Gamma) \left(\frac{V}{V_0} \right)^{1/6} \left(\frac{B_{\text{sta}}}{B_0} \right)^{1/2} \left(1 - \frac{2 P_{\text{sta}}}{3 B_{\text{sta}}} \right), \quad (8)$$

where $\omega_i^0(\Gamma)$ is the optical phonon frequency in equilibrium volume at gamma point which is calculated by Quantum Espresso package.

Thus, non-equilibrium functional Gibbs free energy can be minimised in proportion to volume.

$$\left[\frac{\partial G^*(V; P, T)}{\partial V} \right] = 0. \quad (9)$$

By solving the above equation, heat capacity at constant volume and pressure are obtained as

$$C_V = \underbrace{12 N k_B D \left(\frac{\theta_{\text{DE}}}{T} \right) - \frac{9 N k_B (\theta_{\text{DE}}/T)}{e^{\theta_{\text{DE}}/T} - 1}}_{C_{V\text{ac}}}$$
$$+ \underbrace{n k_B \sum_{j=1}^{3N-3} \frac{(\omega_j/T)^2 \, e^{\omega_j/T}}{\left(e^{\omega_j/T} - 1 \right)^2}}_{C_{V\text{opt}}}, \quad (10)$$

$$C_p = \left(\frac{\partial H}{\partial T} \right)_p. \quad (11)$$

3. Results and discussions

3.1 *Structural properties*

Structural properties of $Al_x Ga_{1-x} As$ are obtained by fitting energy–volume data with linear Brich–Murnaghan equation of state. Variations of lattice constant vs. percentage of Al concentration for $Al_x Ga_{1-x} As$ are shown in figure 1. Experimental values of lattice constant for AlAs and GaAs and other theoretical values are also shown for comparison. Obtained values of lattice constant in the present work are a little lower than experimental values but have a good agreement with experimental and theoretical results. This difference is originated from exchange-correlation function used in the present work (LDA) and Mao *et al* [1] calculations (GGA).

Present results have a positive and small deviation from straight line, and follows Vegard's law. It should be noted that the value of deviation from the linear state depends on factors including: the relative size of the constituent elements, the relative volume per valence electron, Brillion-zone effects and electrochemical differences between the elements. This deviation can be
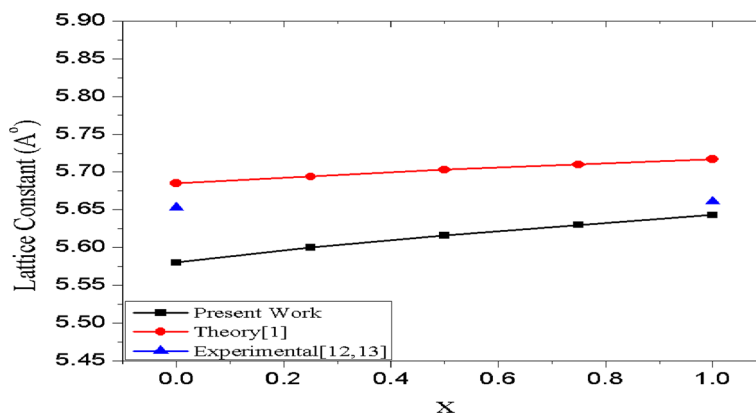
Figure 1. Variations of lattice constant vs. concentration of Al in $Al_x Ga_{1-x}As$ compounds.
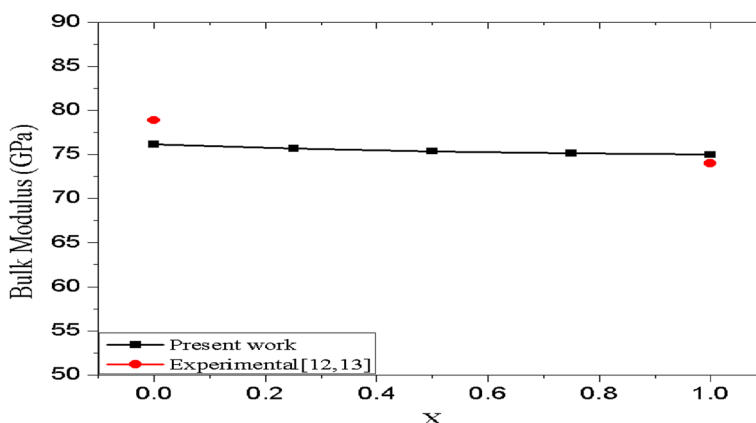

Figure 2. Bulk modulus vs. different values of x and their comparison by experimental values.

due to covalent radius of atoms of group III and unit cell volume. Covalent radii of Al and Ga are respectively 1.21 Å and 1.22 Å. For very small values of $|r_M - r_N|$, a very small positive deviation from Vegard's law is predicted [7]. In figure 2, the variations of bulk modulus of $Al_x Ga_{1-x}As$ with different values of x are shown.

The variations of volumetric modulus decrease by increasing the percentage of Al in this alloy, which is consistent with the experiment.

In table 1, values of lattice constant and bulk modulus for different percentages of Al concentration are shown. Unfortunately, experimental values are not available for lattice constant and bulk modulus for $x = 0.25, 0.5, 0.75$, but results for $x = 0.0, 1.0$ have a good consistency with experimental and theoretical results.

3.2 *Phonon calculation*

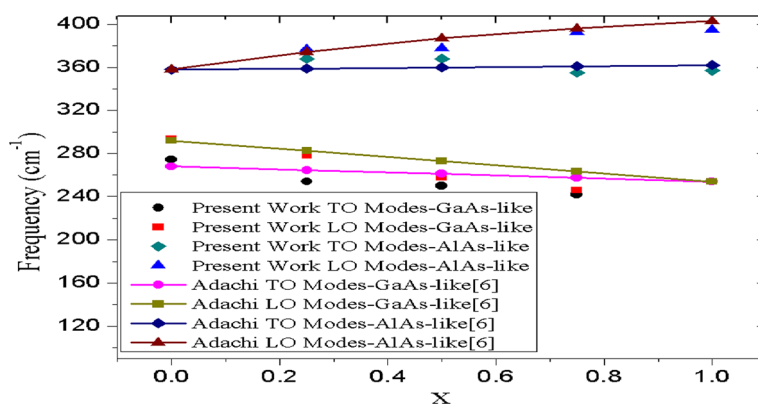For obtaining thermal properties, optical phonon frequency modes at gamma point are required. In figure 3, the obtained values of the present work and by Adachi [6] are shown which are on the experimental basis. $Al_x Ga_{1-x}As$ has two pairs of longitude optical (LO) modes and transverse optical (TO) modes which are called GaAs-like and AlAs-like modes. GaAs-like (AlAs-like) modes have phonon frequencies that are related to bulk GaAs (AlAs). GaAs and AlAs are polarised heterojunction semiconductors.

In these crystals, interatomic forces include Coulomb long-range interactions and this is due to the partial ionic nature of their chemical bonding. These polarised heterojunction semiconductors have TO–LO splitting at gamma point and this splitting is because of the long-range nature of interatomic forces which is visible in figure 3 and is related to the breaking of cubic symmetry for the accompaniment induced dipoles with vibration modes.

As can be seen, with increasing concentration of Al atoms, optical mode frequencies of AlAs-like modes increase and frequencies of GaAs-like modes decrease. TO–LO splitting is due to the difference of electronegativity between Al and As atoms and as a result, their polarity is higher than AlAs-like modes compared to GaAs-like modes.

Table 1. Comparison of values obtained from the present work with other theoretical and experimental works for bulk modulus and lattice constant for different values of x in $Al_xGa_{1-x}As$ alloy.

Experimental bulk modulus [12,13]	Bulk modulus for the present work	Lattice constant for other theoretical work [1]	Lattice constant for the present work	Experimental lattice constant [12,13]	Concentration of Al
78.9	76.14	5.685	5.580	5.653	0
	75.71	5.694	5.600		0.25
	75.37	5.703	5.616		0.5
	75.13	5.710	5.630		0.75
74	74.97	5.717	5.643	5.661	1

Figure 3. Phonon mode frequency of $Al_xGa_{1-x}As$ for different values of x.
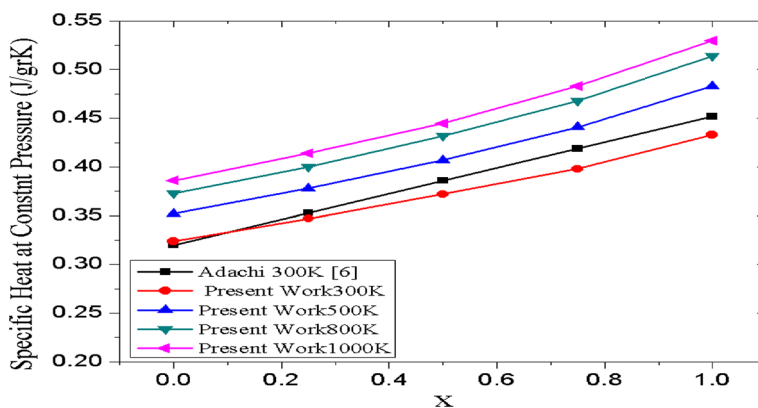
Figure 4. Variations of specific heat at constant pressure for different values of Al concentration in $Al_xGa_{1-x}As$ alloy.

3.3 *Thermal properties*

Figure 4 shows the plots of specific heat at constant pressure C_p vs. concentration x for temperatures 300, 500, 800 and 1000 K. The results obtained from interpolation of specific heat at constant pressure for bulk AlAs and GaAs by Adachi [6] at 300 K are in good agreement with the present work at 300 K. Also, linear variations can be seen for different temperatures.

Figure 5 shows the variations of specific heat at constant volume for $x = 0.0, 0.25, 0.5, 0.75, 1$. It can

be seen that the variation of specific heat at constant volume in low temperature has a T^3 behaviour while for higher temperatures it converges to the saturation limit. As shown in the figure, specific heat at constant volume increases with increasing x.

The materials which have stronger bonding and lower molecular mass have higher specific heat. Ga has higher electronegativity than Al and so the difference of electronegativity in AlAs is higher than GaAs. So it is more polarised and has stronger bonding. Because of the stronger bonding and lower molecular
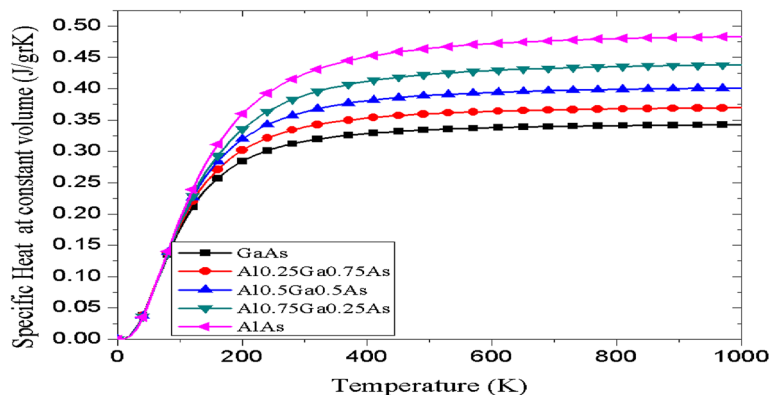
Figure 5. Variation of specific heat at constant volume vs. temperature for $Al_xGa_{1-x}As$.
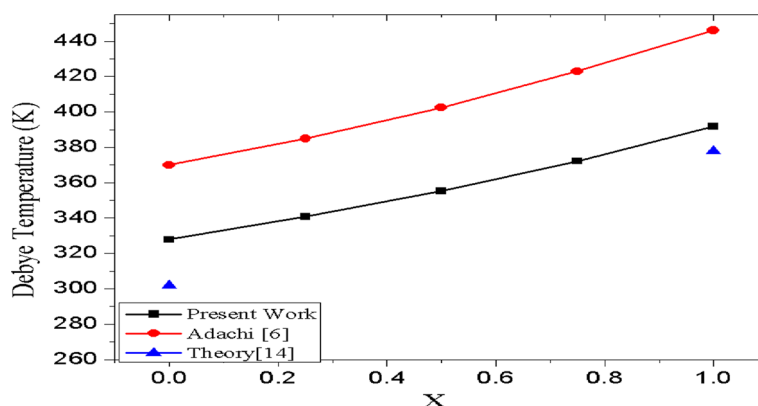

Figure 6. Variations of Debye temperature for different values of Al concentration in $Al_xGa_{1-x}As$ alloy.

mass of AlAs, by increasing x and increasing Al concentration, specific heat increases.

Figure 6 shows Debye temperature T_D vs. x. Present results are compared with interpolation work by Adachi [6] and other theoretical work [14] for AlAs and GaAs. For lower x, as the number of Al atoms decrease, and Al atoms are lighter than Ga atoms, their frequency and so cut-off frequency increase leading to increase in Debye temperature with x.

variation of specific heat at constant volume in low temperature has a T^3 behaviour while for higher temperatures it converges to the saturation limit. Also the variation of specific heat at constant pressure and Debye temperature with Al concentration indicate that both C_p and T_D increase by increasing Al in $Al_xGa_{1-x}As$ alloy.

4. Conclusion

In this paper, structural and thermal properties of $Al_xGa_{1-x}As$ alloy are investigated for different values of x ($x = 0.0, 0.25, 0.5, 0.75, 1.0$) using quasiharmonic Debye–Einstein model. Correction of Vegard's law for lattice constant was investigated. There is a little deviation in lattice constant diagram vs. x which can be related to low and positive difference of covalent radius of Al and Ga atoms. The obtained values of specific heat at constant volume showed that the

References

[1] Y Mao, X X Liang, G J Zhao and T L Song, *2nd Int. Conf. Math. Model. Phys. Sci.* **490**, 12172 (2014)

[2] F El Haj Hassan, A Breidi, S Ghemid, B Amrani, H Meradji and O Pagès, *J. Alloys Compd.* **499**, 80 (2010)

[3] F K Boz, B Nisanci, S Aktas and S Erol Okan, *Appl. Surf. Sci.* **387**, 76 (2016)

[4] R K Nayak, S Das, A K Panda and T Sahu, *Superlatt. Microstruct.* **38**, 75 (2015)

[5] P V Seredin, A S Lenshin, I N Arsentiev and I S Tarasov, *Mater. Sci. Semicond. Process.* **38**, 107 (2015)

[6] S Adachi, *GaAs and related materials* (World Scientific Publishing Co. Pvt. Ltd, 1999)

[7] S T Murphy, A Chroneos, C Jiang, U Schwingenschlög and R W Grimes, *Phys. Rev. B* **82**, 073201 (2015)

[8] M A Blanco, E Francisco and V Luaña, *Comput. Phys. Commun.* **158**, 57 (2004)

[9] A Otero-de-la-Roza and V Luaña, *Comput. Phys. Commun.* **182**, 1708 (2011)

[10] A Otero-de-la-Roza, D Abbasi-Pérez and V Luaña, *Comput. Phys. Commun.* **182**, 2232 (2011)

[11] P Giannozzi *et al*, *Condens. Matter* **21**, 395502 (2009)

[12] R G Greene, H Luo, T Li and A L Ruoff, *Phys. Rev. Lett.* **72**, 2045 (1994)

[13] J S Blakemore, *J. Appl. Phys.* **53(10)**, R123 (1982)

[14] C Toher, J J Plata, O Levy, M de Jong, M Asta, M B Nardelli and S Curtarolo, *Phys. Rev. B* **90**, 174107 (2014)